

## Growth of Co on a stepped and on a flat Cu(001) surface

U. Ramsperger, A. Vaterlaus, P. Pfäffli, U. Maier, and D. Pescia

*Laboratorium für Festkörperphysik, Mikrostrukturforschung, Eidgenössische Technische Hochschule-Hönggerberg,  
8093 Zürich, Switzerland*

(Received 2 October 1995)

The growth of Co on Cu(001) is investigated with scanning tunneling microscopy (STM), Auger electron spectroscopy, and low-energy electron diffraction. Island shape and size differs drastically for Co evaporated onto a flat or a stepped Cu(001) surface. Deviations from ideal layer-by-layer growth are small. Evaporating at 540 K results in an island free surface, annealing to 495 K induces depressions into the Co islands but does not change their shape and arrangement. A retarding field Auger system and an Auger spectrometer with cylindrical mirror analyzer are calibrated simultaneously with the help of the STM.

### I. INTRODUCTION

Magnetic properties are very sensitive to structural details. It was found that Co grown on a flat Cu(001) surface is magnetized along the  $[\pm 110]$  directions. Grown on a stepped surface, Co exhibits a uniaxial easy axis along the steps.<sup>1-3</sup> This easy direction of the magnetization is rotated by  $90^\circ$  through the deposition of a minute amount of Cu on top of the Co.<sup>4</sup> This demonstrates the dependence of the magnetic properties on the symmetry<sup>5</sup> and the morphology.<sup>6</sup> The present paper describes the growth of Co on a stepped and a flat Cu(001) crystal.

Co grows in the fcc phase with a small tetragonal distortion ( $<4\%$ ) along the surface normal.<sup>7,8</sup> A bilayer growth mode was reported for the initial two atomic layers (AL). Thereafter Co grows in a perfect layer-by-layer mode.<sup>9,10</sup> The nonperfect initial growth was detected with scanning tunneling microscopy (STM),<sup>9</sup> angle-resolved x-ray photoemission scattering,<sup>11</sup> and x-ray diffraction.<sup>12</sup>

The STM measurements presented in this paper show that the growth mode of Co on Cu(001) depends crucially on the surface condition of the substrate. On a stepped surface (miscut  $3.4^\circ$ ) with step orientation along the  $[110]$  direction we find an irregular arrangement of the Co islands with their shape changing as a function of film thickness. Regularly shaped two-dimensional islands are found on a flat Cu substrate (miscut  $0.2^\circ$ ). Their size and arrangement changes with a period of 1 AL. This means that a 2.5 AL film looks identical to a 3.5 AL film. Both growth modes are observed simultaneously for a Cu substrate having stepped and flat surface areas.

For Co grown on the flat crystal we do not observe the degree of bilayer growth reported in the literature.<sup>9,11,12</sup> Possible reasons for this discrepancy are discussed below.

An Auger system with a retarding field analyzer (RFA) and one with a cylindrical mirror analyzer (CMA) are calibrated simultaneously with the help of the STM. A mean free path of 9.9 Å is found for the high-energy Co and Cu Auger electrons.

Evaporating Co at substrate temperatures up to 430 K does not change the shape and the arrangement of the Co islands but induces depressions into them. This changes dras-

tically at 540 K. For this temperature we find an island free and flat surface.

### II. EXPERIMENT

All experiments described in the following have been done in a new UHV system consisting of three chambers. Samples and tips are introduced through a load lock into the preparation chamber. Surface cleaning, film growth, and surface characterization with low-energy electron diffraction (LEED) and Auger spectroscopy is done in this chamber. Auger spectra can be collected by using a RFA or a CMA. After preparation the samples are transferred to the Kerr chamber for spatially resolved Kerr effect measurements or to the STM chamber for the structural characterization. All three chambers are independently pumped and have a base pressure better than  $5 \times 10^{-11}$  mbar.

Chemically etched tungsten tips are used for the STM imaging. After insertion into the vacuum the tips are heated by electron bombardment (600 V, 3–6 mA) and characterized by field emission. Only tips with a field emission threshold of about 300 V were used for STM imaging (typically 0.1 nA at 300 V).

The Cu(001) crystals were mechanically polished down to a grain size of 1  $\mu\text{m}$ . This was followed by electropolishing using a solution with 30% of  $\text{HNO}_3$  in  $\text{CH}_3\text{OH}$ . During a few seconds a positive voltage of about 3 V was applied to the crystal. This procedure resulted in a mirrorlike Cu(001) surface. Electropolishing was found to be crucial in order to get a clean, flat, and well-ordered surface.

After insertion into the vacuum system the samples were cleaned by Ar ion sputtering using a beam energy of 500 V and a target current of 7  $\mu\text{A}$ . This was followed by annealing the sample up to 770 K during a few hours. Annealing to higher temperatures results in a S-covered Cu surface. Repeating this procedure about five times resulted in a clean surface showing sharp LEED spots. For the last cycle the sample was sputtered during 5 min and annealed to 720 K during 15 min. Figures 1(a) and 1(b) show typical surface areas of the flat and the stepped Cu(001) crystal. The average distance between steps amounts to 500 Å for the flat and 30 Å for the stepped crystal. The gradient enhanced image 1(c)

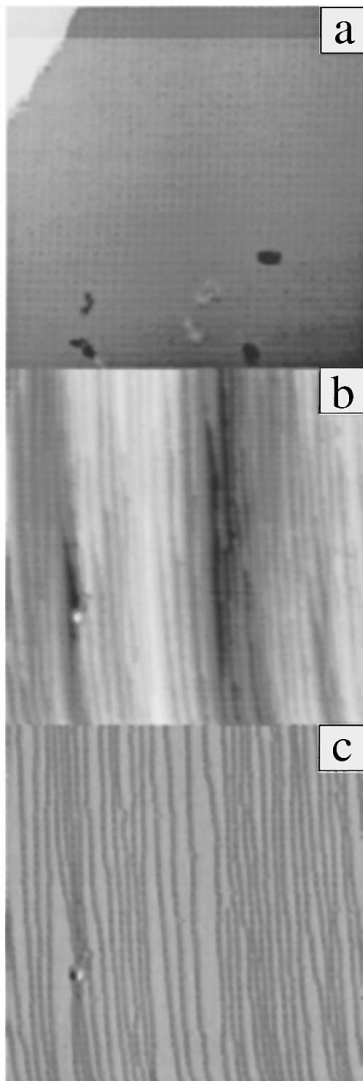


FIG. 1. (a)  $1000 \text{ \AA} \times 1000 \text{ \AA}$  STM topograph of the flat Cu(001) surface. The  $[-110]$  direction is along the horizontal axis of the image. Gray scale range:  $2.1 \text{ \AA}$ . Tunnel current:  $0.2 \text{ nA}$ . Sample voltage:  $0.38 \text{ V}$ . (b)  $930 \text{ \AA} \times 930 \text{ \AA}$  STM topograph of the stepped Cu(001) surface. The  $[-110]$  direction is along the horizontal axis of the image. Gray scale range:  $5.6 \text{ \AA}$ . Tunnel current:  $0.2 \text{ nA}$ . Sample voltage:  $0.96 \text{ V}$ . (c) Gradient enhanced image showing the same area as (b).

shows the same area as Fig. 1(b). Steps appear as dark lines and the terraces appear gray.

All STM images shown in the following have been collected using a home-built STM having a coarse positioning ability along both surface directions. Details of the apparatus will be described in a forthcoming publication. The STM was calibrated by imaging GaAs with atomic resolution.

Co was evaporated from a Knudsen cell type evaporation source. An evaporation rate of  $0.2$  up to  $0.4 \text{ AL/min}$  was used to produce the layers described in the following. During evaporation the pressure rose typically up to  $5 \times 10^{-10} \text{ mbar}$ .

### III. Co GROWN ON THE STEPPED AND ON THE FLAT Cu(001) SUBSTRATE

Depositing the same amount of Co onto the flat and the stepped Cu crystal results in layers having a completely dif-

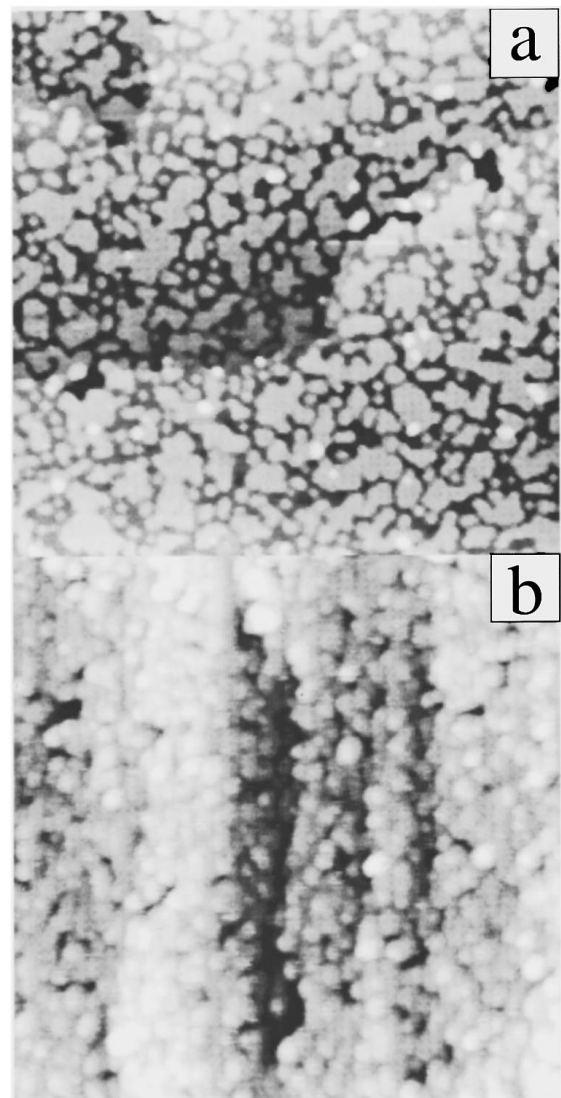


FIG. 2.  $1000 \text{ \AA} \times 1000 \text{ \AA}$  STM topograph of a  $0.5 \text{ AL}$  Co film deposited onto the flat Cu(001) surface (a) and onto the stepped Cu(001) surface (b). Note the two steps crossing image (a). The  $[-110]$  direction is along the horizontal axis of the image. Gray scale range:  $4.2 \text{ \AA}$  (a) and  $6.5 \text{ \AA}$  (b). Tunnel current:  $0.1 \text{ nA}$  (a) and  $0.2 \text{ nA}$  (b). Sample voltage:  $0.4 \text{ V}$ .

ferent surface morphology. The well-separated islands of a  $0.5 \text{ AL}$  Co film on the flat crystal [Fig. 2(a)] have a preferential edge orientation along the  $[\pm 110]$  direction (see also Fig. 5). The diameter of the islands varies from  $10 \text{ \AA}$  up to  $250 \text{ \AA}$ . On the stepped surface the islands appear to be round [Fig. 2(b)]. They have a diameter ranging from  $20 \text{ \AA}$  up to  $50 \text{ \AA}$ . For this surface it is impossible to recognize the layer to which a single Co island belongs. The arrangement seems to be arbitrary and only the direction of the underlying Cu steps can still be recognized. We find that the topographs shown in Fig. 2 are typical for this coverage. Identical images have been collected at different spots on the surface and on other layers having the same thickness. The Auger spectra for the two samples are identical.

Increasing the coverage from  $0.5$  to  $2 \text{ AL}$  [Fig. 3(a)] results in a perfect Co film with almost no Co in the third layer. Evaporating the same amount of Co onto the stepped sub-

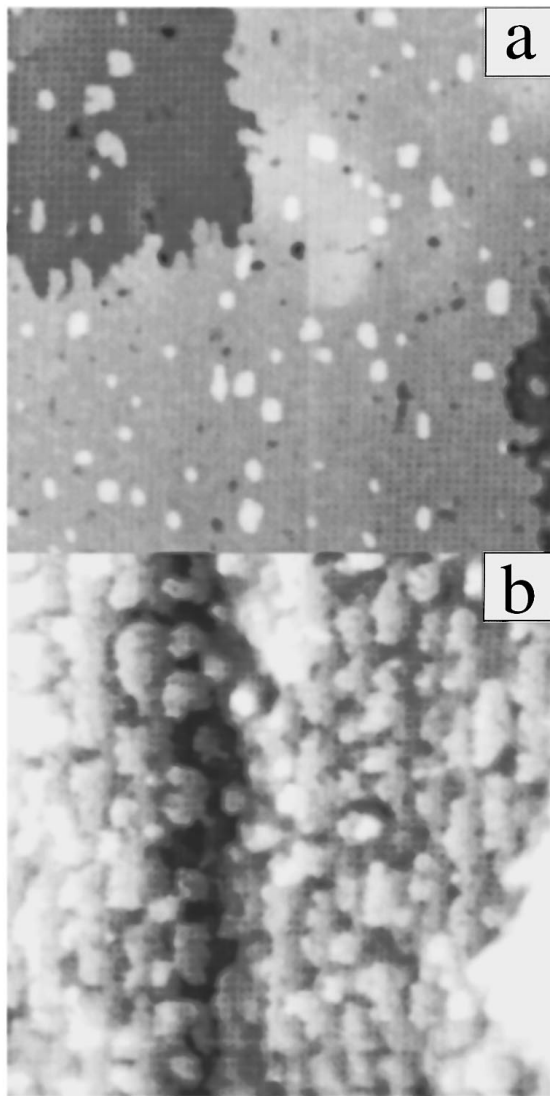


FIG. 3. STM topograph of 2.0 AL of Co deposited onto the flat (a) and onto the stepped (b) Cu crystal. The  $[-110]$  direction is along the horizontal axis of the image. The image size is 1000 and 500 Å, respectively. Gray scale range: 5.4 Å and 6.9 Å (b). Tunnel current: 0.2 nA. Sample voltage: 0.6 V.

strate gives the topograph shown in Fig. 3(b). If the growth is layer by layer, the Co should reproduce the topographic properties of the substrate exactly. This is not the case. The topograph in Fig. 3(b) shows Co patches that are extended along the steps of the substrate. Identical Auger spectra are obtained for the Co layers shown in Figs. 3(a) and 3(b).

The nonregular appearance of the layer grown on the stepped crystal is underlined in Fig. 4. It arises from the fact that straight Cu steps transform into meandering steps of the Co layer grown on top. Figure 4 shows some isolated steps of the 2 AL Co film grown on the flat substrate. The steps are not straight but are meandering with an amplitude of about 70 Å. This fluctuating deviation between the Co step position and the position of the underlying Cu step results in a modulation of the film thickness in this region. Therefore the layer-by-layer growth is obscured by the presence of steps. Note that the distance between the steps of the second crystal is smaller than the modulation amplitude of the Co step po-

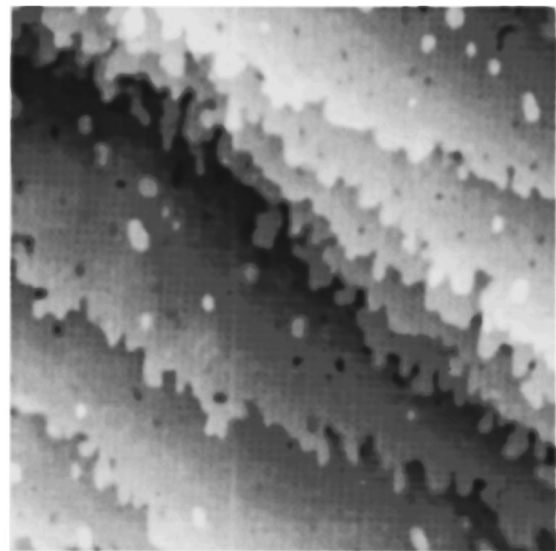


FIG. 4. STM topograph of 2.0 AL Co deposited onto the flat Cu(001) crystal. The  $[-110]$  direction is along the horizontal axis of the image. The image size is 1000 Å. Gray scale range: 7.4 Å. Tunnel current: 0.2 nA. Sample voltage: 0.6 V.

sition. Consequently the growth on this crystal is completely step dominated. The distance of the steps visible in Fig. 4 is becoming small in the upper left corner of the image. This region simulates the stepped crystal. The surface pattern in this region is very similar to the one shown in Fig. 3(b).

A mean square Co step roughness of 62 Å was calculated from STM topographs of Co grown on Cu(1 1 17).<sup>13</sup> These findings are in agreement with the results described above.

Nothing new is found if the coverage on the flat crystal is increased. The same island pattern is very well reproduced for each new atomic layer. This means that a 2.5 AL film looks identical to a 3.5 AL film, an observation that is in agreement with Ref. 9. However, for the stepped Cu surface the island shape and size change with coverage. It is not possible to separate the Co belonging to different atomic layers. It is impossible to detect the completion of a layer by imaging the Co on the stepped surface. Just by depositing the same amount of Co onto the flat crystal gives the right calibration of the thickness.

#### IV. THE FIRST LAYERS

Much debate arose about the growth of the first two layers of Co on Cu(001). A perfect layer-by-layer growth was reported based on LEED and Auger measurements.<sup>7</sup> From angle-resolved x-ray photoemission scattering experiments it was claimed that cobalt initially forms two layer thick islands.<sup>11</sup> A significant concentration of Co islands of bilayer height for a coverage above 0.5 AL was found using x-ray diffraction.<sup>12</sup> A STM experiment showed that 0.1 AL of Co are already in the second layer after having deposited 0.8 AL.<sup>9</sup> STM is the most direct method for studying initial growth modes. The covered area and the thickness of the islands is directly measured from a topographic image. Scattering methods require an absolute calibration of the thickness in order to correlate it with the onset of scattering from

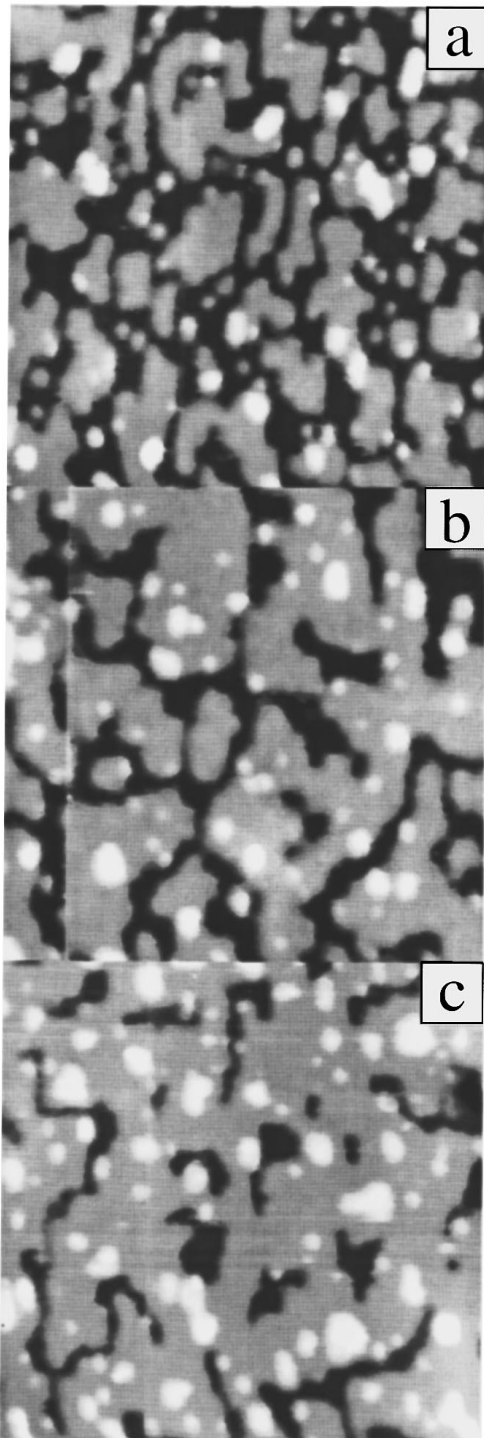


FIG. 5. STM topographs of 0.55 AL (a), 0.63 AL (b), and 0.91 AL (c) of Co grown on the flat Cu(001) crystal. Black corresponds to the Cu substrate, gray to the first layer, and white to the second layer of Co. The image size is 500 Å, 400 Å, and 500 Å, respectively. Tunnel current: 0.1 nA. Sample voltage:  $-0.4$  V. The gray scale range for the images (a)–(c) is equal to 4.3, 4.6, and 5.6 Å. The  $[-110]$  direction is along the horizontal axis of the image.

the second layer. A calibration done with an Auger or with a quartz microbalance can be off by a factor of two (see Sec. V). Furthermore the presence of steps can result in a modulation of the film thickness (see previous section). All this could result in a wrong interpretation of the scattering experiment.

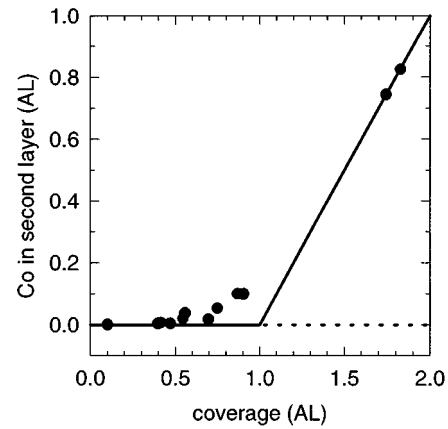


FIG. 6. The amount of Co found in the second layer is plotted as function of the coverage. Each point was obtained by analyzing the pixel height distribution of the corresponding STM image. The solid line corresponds to the ideal layer-by-layer growth mode.

Figure 5 shows STM topographs taken in the critical range from 0.6 AL up to 0.9 AL. This is the range where a significant bilayer growth mode should be observed. The height distribution of the image pixels is used to determine the amount of Co in the first and the second layer. The result of this analysis for the layers shown in Fig. 5 and for other layers is shown in Fig. 6. The amount of Co found in the second layer is plotted as a function of the amount of Co deposited. The solid line indicates the behavior that would be found for an ideal layer-by-layer growth mode. Figure 6 shows that the degree of bilayer growth observed is much smaller than the one reported in the literature.<sup>11,12</sup> Less than 10% of the Co atoms are found in the second layer for a film with a nominal thickness of 0.9 AL. This deviation from the ideal layer-by-layer growth mode is smaller but close to the one reported in Ref. 9.

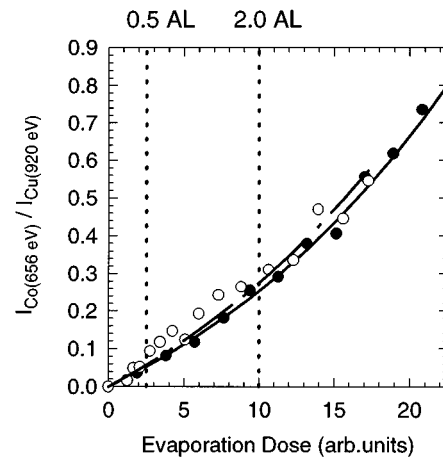


FIG. 7. Intensity of the Co 656-eV Auger line divided by the intensity of the Cu 920-eV line plotted as function of the evaporation dose. Filled circles are measured with a cylindrical mirror electron energy analyzer, the open circles with a retarding field electron energy analyzer. The lines are a fit to the measured points (see text). The evaporation dose was calibrated with the help of the STM at a coverage of 0.5 and 2.0 AL (indicated by the dotted lines).

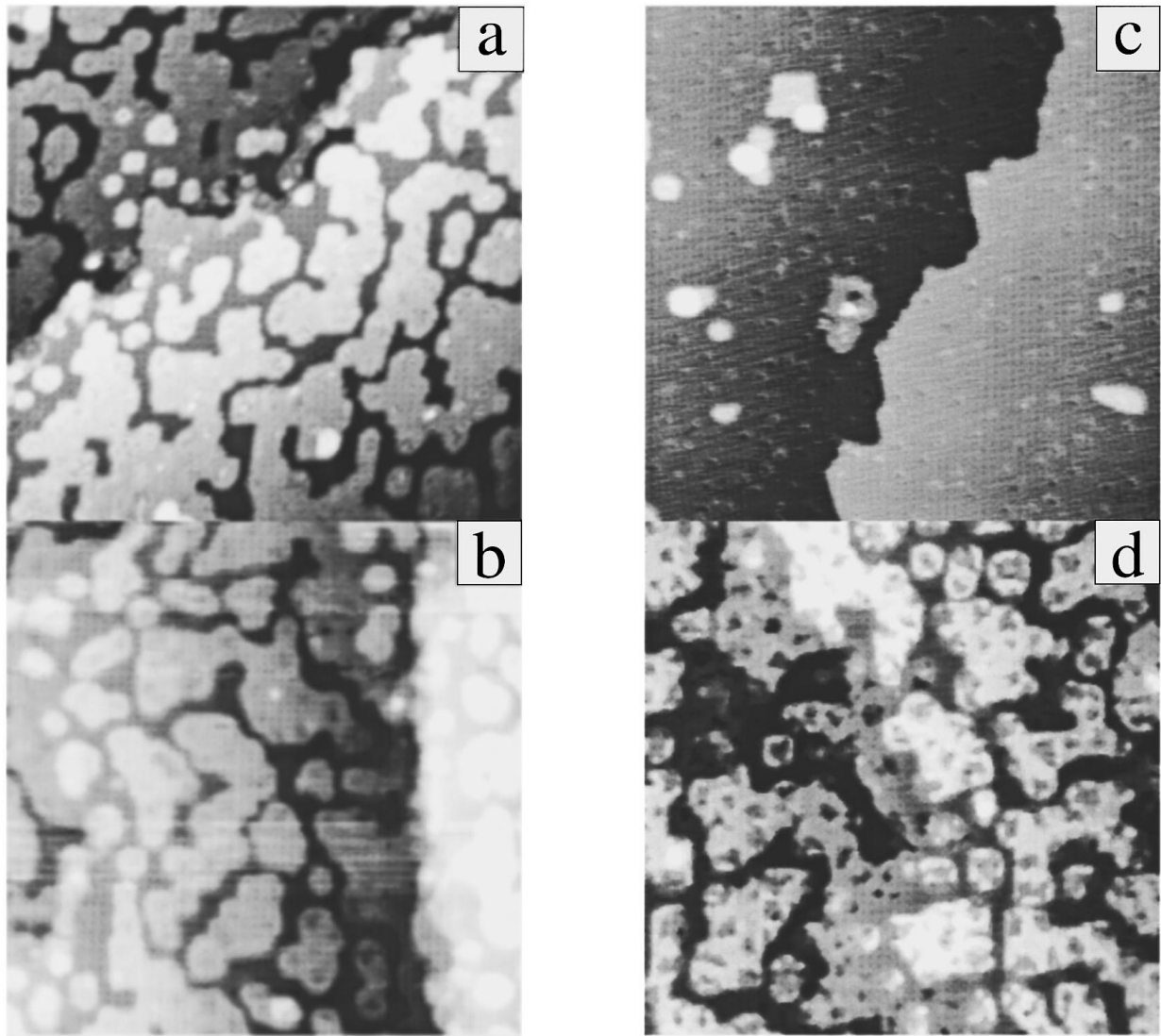


FIG. 8. STM topographs of 0.7 AL of Co grown at 370 K (a), 430 K (b), and 540 K (c). The layer shown in (d) was grown at room temperature and subsequently annealed to 495 K during 450 s. The  $[-110]$  direction is along the horizontal axis of the image. The image size is 500 Å. Tunnel current: 0.1 nA. Sample voltage:  $-0.4, 0.4, 1.05,$  and  $0.92$  V. The gray scale range is 5.6, 4.7, 3.6, and 3.2 Å.

## V. CALIBRATION OF THE RFA AND THE CMA AUGER

Film thickness calibration is often done with the help of Auger spectroscopy. Calculating a film thickness from Auger spectra requires the knowledge of the mean free path of the electrons. Furthermore it has to be taken into account that a RFA collects electrons that are emitted with an angle ranging from 0 up to  $50^\circ$  measured from the surface normal of the samples whereas the CMA just accepts electrons emitted with  $42^\circ$ . Therefore the Auger thickness calibration has to take all this into account.

The ratio of the Co Auger peak at 656 eV and the Cu Auger peak at 920 eV is plotted in Fig. 7 as function of the Co evaporation dose. The filled circles are measured with the CMA (Ref. 14) the open circles with the RFA.<sup>15</sup> By counting the coverage with the help of an STM topograph we can transform the evaporation dose scale into an absolute atomic layer scale. This was done for a 0.5 AL and a 2 AL film. The two STM calibration points give the absolute thickness scale and confirm the linearity of the thickness versus evaporation

dose. Setting for simplicity the mean free path of the Cu 920-eV Auger electrons equal to the mean free path of the Co 656-eV electrons leads to the following formula for the Auger ratio:

$$I_{\text{Co}}/I_{\text{Cu}}(d) = I_{\text{Co}}^0/I_{\text{Cu}}^0[\exp(d/\lambda) - 1].$$

Here  $d$  is the layer thickness,  $I_{\text{Co}}^0$  is the Co Auger signal from a very thick Co layer, and  $I_{\text{Cu}}^0$  is the Cu signal from a clean Cu surface.  $\lambda$  is the only adjustable parameter. The solid lines in Fig. 7 are calculated using  $\lambda = 4.3 \pm 2.1$  and  $4.1 \pm 0.5$  AL for the RFA and for the CMA Auger respectively.  $I_{\text{Co}}^0/I_{\text{Cu}}^0$  is 0.47 for the RFA and 0.40 for the CMA. The mean free path  $\lambda$  deduced from the CMA measurements equals  $\lambda/\cos 42^\circ$ . Therefore we get 5.5 AL (9.9 Å) for  $\lambda$ . This value is smaller than the 6.5 and 7.8 AL obtained for the 656- and 920-eV electrons, respectively, using the commonly accepted “universal curve.”<sup>16</sup> It is difficult to deduce a mean free path

from the RFA measurements since not all the emission angles have the same weight.<sup>17</sup>

## VI. ELEVATED SUBSTRATE TEMPERATURES

The influence of the substrate temperature on film growth is investigated by depositing the same amount of Co onto the Cu held at 370, 430, and 540 K. The topographs of the corresponding layers are shown in Figs. 8(a)–(c). The coverage equals 0.7 AL. Small depressions evolve for a growth temperature of 370 K. They are 0.2 Å deep and are irregularly arranged. Shape and arrangement of the Co islands remain unaffected. Those depressions become more pronounced for a substrate temperature of 430 K. Note that Co and Cu can be distinguished in Fig. 8(b) since the depressions are found on the Co islands and not on the Cu substrate visible in between the islands. The depressions could be caused by missing Co atoms, by interdiffusion, or by imperfections of the underlying substrate. We always observe empty Cu sites on a flat Cu surface. Under normal growth conditions these vacancies must be filled with Co atoms in order to allow the growth of flat Co islands. Those Co atoms repairing the substrate are embedded into a Cu layer and are therefore very attractive for interdiffusion. This could be the reason for the depressions visible in Figs. 8(a) and 8(b). However, the density of missing Cu atoms is not as high as the density of depressions. This can be seen in Fig. 8(b) since the uncovered regions appear to be flat.

Growing Co at a substrate temperature of 540 K gives a completely new surface morphology [Fig. 8(c)]. We find a flat and almost island free surface. Co was proposed to diffuse into the Cu at a temperature of 670 K.<sup>11</sup> Heating a 3 AL Co film up to 490 K resulted in a layer with a few big holes<sup>18</sup> but with an arrangement of Co islands being similar to the room temperature grown layer. The question that arises therefore is: Do we see a perfect Co layer or Cu covered Co in Fig. 8(c)?

An identical amount of Co was deposited for the layers shown in Fig. 8. Consequently the Auger peak ratio for Co

and Cu should be constant for all three layers. The Auger peak ratio is defined as the intensity of the Co 656-eV Auger line divided by the intensity of the Cu 920-eV Auger line. For images 8(a), 8(b), and 8(c) we find ratios of 0.086, 0.060, and 0.056. Extending formula 1 to the bilayer system and calculating the Auger ratio for a 0.7 AL film and a 0.7 AL film covered with Cu gives 0.082 and 0.066, respectively. Therefore the Auger spectrum suggests the top layer of Fig. 8(c) to be Cu.

Annealing a room temperature grown Co layer during 450 s to 495 K gives the topograph shown in Fig. 8(d). After annealing the Co exhibits depressions similar to the layer grown at 430 K.

## VII. DISCUSSION

In conclusion, STM imaging shows that the quality of the layer-by-layer growth of Co on a flat Cu(001) surface is high. Island shape and size reproduce very well for Co grown on a flat substrate. For room temperature deposition we find flat Co islands with a preferential step orientation along the  $[\pm 110]$  direction. Co deposited onto a stepped Cu surface gives a layer that largely but not exactly reproduces the steps of the underlying substrate. The islands are extended along the step direction and are not as regularly shaped as the Co islands found on a flat crystal.

Notice that detecting a bilayer growth mode from scattering experiments alone is very difficult. An absolute thickness calibration, which only the STM can provide, is required. The influence of the growth rate on film quality and magnetic properties will be described in a forthcoming publication.

## ACKNOWLEDGMENTS

We thank C. H. Back and C. Würsch for the CMA measurements displayed in Fig. 5, R. Allenspach and W. Weber for the stepped Cu crystal, and all of them for many stimulating discussions. Financial support from the Swiss National Fond is gratefully acknowledged.

<sup>1</sup>A. Berger, U. Linke, and H. P. Oepen, *Phys. Rev. Lett.* **68**, 839 (1992).

<sup>2</sup>P. Krams, F. Lauks, R. L. Stamps, B. Hillebrands, G. Güntherodt, and H. P. Oepen, *J. Magn. Magn. Mater.* **121**, 483 (1993).

<sup>3</sup>P. Krams, B. Hillebrands, G. Güntherodt, and H. P. Oepen, *Phys. Rev. B* **49**, 3633 (1994).

<sup>4</sup>W. Weber, C. H. Back, A. Bischof, D. Pescia, and R. Allenspach, *Nature* **374**, 788 (1995).

<sup>5</sup>L. Néel, *J. Phys. Radium* **15**, 225 (1954).

<sup>6</sup>D. S. Chuang, C. A. Ballentine, and R. C. O'Handley, *Phys. Rev. B* **49**, 15 084 (1994).

<sup>7</sup>A. Clarke, G. Jennings, R. F. Willis, P. J. Rous, and J. B. Pendry, *Surf. Sci.* **187**, 327 (1987).

<sup>8</sup>O. Heckmann, H. Magnan, P. le Fevre, D. Chandris, and J. J. Rehr, *Surf. Sci.* **312**, 62 (1994).

<sup>9</sup>A. K. Schmid and J. Kirschner, *Ultramicroscopy* **42-44**, 483 (1992).

<sup>10</sup>J. J. de Miguel, A. Cebollada, J. M. Gallego, R. Miranda, C. M. Schneider, P. Schuster, and J. Kirschner, *J. Magn. Magn. Mater.* **93**, 1 (1991).

<sup>11</sup>Hong Li and B. P. Tonner, *Surf. Sci.* **237**, 141 (1990).

<sup>12</sup>S. Ferrer, E. Vlieg, and I. K. Robinson, *Surf. Sci. Lett.* **250**, L363 (1991).

<sup>13</sup>M. Giesen, F. Schmitz, and H. Ibach, *Surf. Sci.* **336**, 269 (1995).

<sup>14</sup>Perkin Elmer Model 10-155A Cylindrical Mirror Analyzer.

<sup>15</sup>Omicron Retarding Field Analyzer Model SPEC4.

<sup>16</sup>M. P. Seah and W. A. Dench, *Surf. Interface Anal.* **1**, 2 (1979).

<sup>17</sup>W. F. Egelhoff, *Crit. Rev. Solid State Mater. Sci.* **16**, 213 (1990).

<sup>18</sup>A. K. Schmid, D. Atlan, H. Itoh, B. Heinrich, T. Ichinokawa, and J. Kirschner, *Phys. Rev. B* **48**, 2855 (1993).